PHYSICAL REVIEW B VOLUME 43, NUMBER 4 1 FEBRUARY 1991

Neutron-irradiation effects on critical current densities in single-crystalline $YBa_2Cu_3O_{7-\delta}$

F. M. Sauerzopf, H. P. Wiesinger, W. Kritscha, and H. W. Weber
Atominstitut der Österreichischen Universitäten, A-1020 Wien, Austria

G. W. Crabtree
Materials Science Division, Argonne National Laboratory, Argonne, Illinois 60439

J. Z. Liu
Department of Physics, University of California, Davis, California 95616
(Received 6 April 1990; revised manuscript received 7 June 1990)

Neutron-irradiation experiments were made on two high-quality $YBa_2Cu_3O_{7-\delta}$ single crystals in the fluence range from 2×10^{21} to 2×10^{22} m^{-2} ($E>0.1$ MeV). Critical current densities J_c and volume-pinning forces P_V were obtained from magnetization measurements in the temperature range from 5 to 77 K, for magnetic fields up to 8 T, and for field orientations parallel and perpendicular to the crystallographic c direction. All evaluations were made on the basis of an extended anisotropic Bean model. The results show large enhancements of flux pinning, in particular at low neutron fluences, a strong reduction of J_c anisotropy, and significant changes of the temperature dependence of J_c. The complicated (nonlinear) dependence of critical current densities and pinning forces on neutron fluence is discussed in terms of an interaction between the radiation-induced defects with the preirradiation defect structure, based on electron microscopy of individual defects and the defect distribution measured in one crystal after neutron irradiation to 2×10^{22} m^{-2} ($E>0.1$ MeV).

I. INTRODUCTION

Flux pinning and the improvement of critical current densities are considered to be among the most important problems in high-temperature superconductivity at present. Although significant progress has been achieved in ceramic materials,[1-3] experiments on single crystals (or epitaxial thin films) seem to be preferable from a basic point of view because more complete information can be obtained, in particular, on the large contribution of anisotropy effects. In addition, problems related to the weak-link structure of ceramics can be avoided if the single crystals are of sufficient quality, sufficiently homogenized, and fully oxygen treated after the initial growth process.

Based on these considerations, we began investigating single crystals of $YBa_2Cu_3O_{7-\delta}$ as early as 1987 (Ref. 4) and subjected them to fast neutron radiation in order to study the role of radiation-induced defects in the flux-pinning processes of high-T_c superconductors.[5-7] Radiation damage and its effects on flux pinning and critical current densities in conventional superconductors have been investigated in much detail.[8-10] The results show a broad variety of effects and depend to a large extent on the type of material subjected to the radiation (elemental, alloy, or compound superconductors), to the preirradiation defect structures, and, of course, to the type of radiation. In the case of fast neutron irradiation, the primary superconductive properties, such as the transition temperature T_c, are generally not affected very much at relatively low fluences ($\lesssim1\times10^{22}$m^{-2}, $E>0.1$ MeV), but the critical current densities may either increase significantly in low-J_c materials (e.g., Ref. 11) due to the introduction of new pinning centers, or increase because of a radiation-induced increase of H_{c2},[10] or decrease due to an unfavorable interaction with the preirradiation defect structure.[12,13] Hence, neutron irradiation seemed to be an obvious choice for investigating flux-pinning effects in high-T_c single crystals, and actually provided evidence for J_c enhancements very early on.[4-6,14]

However, detailed systematic investigations of the fluence dependence of J_c measured on the same single crystal are scarce,[7] mainly because of the long measuring times needed to investigate magnetization loops and their field, temperature, orientation, and fluence dependence with a SQUID magnetometer. This is in contrast to a variety of neutron-irradiation experiments reported on ceramic superconductors,[15-18] which all showed significant broadening of the hysteretic magnetization loops. However, these results refer to a combination of inter- and intragrain contributions to the measured magnetization loop and were interpreted mainly as reflecting the increasing loss of weak-link behavior with increasing neutron fluence.

In the present paper, we report on a comprehensive study of fast neutron irradiation effects in two high-quality single crystals of $YBa_2Cu_3O_{7-\delta}$ carried out in the fluence range from 2×10^{21} to 2×10^{22} ($E>0.1$ MeV) and covering temperature and magnetic field ranges from 5–77 K and 0–8 T, respectively. Section II is devoted to a description of experimental details and Sec. III to the presentation of results on T_c, J_c, and volume-pinning forces P_v. A discussion of data is presented in Sec. IV, which also relies on recent results of electron microscopic

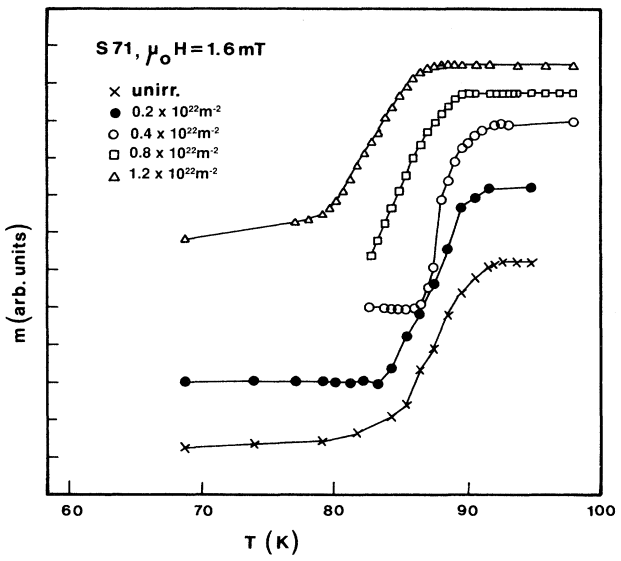

FIG. 1. Transition temperatures measured on sample *S*71 after exposure to various neutron fluences (zero-field cooled to 5 K, warmed up in a field of 1.6 mT).

investigations of one of the single crystals.[19] Finally, our conclusions are drawn in Sec. V.

II. EXPERIMENT

A. Samples

The single crystals were prepared by a flux method[20] and subjected to an extended post-annealing treatment in flowing oxygen. Meissner and shielding measurements in fields as low as 0.1 mT usually showed transition widths of the order of 1–2 K.[21] Two single crystals of the same batch (*S*71, *S*84) were selected for the present experiments. Their physical dimensions, onset T_c's, as well as their transition widths determined from zero-field-cooled magnetization versus temperature curves (in a field of 1.6 mT) are summarized in Table I. (See also Fig. 1). It should be noted that this measuring field, which is the lowest achievable in our system, leads to a certain broadening of the transition curve. Both crystals had a fairly regular rectangular shape but rather rough surfaces, which prevented us from investigating details of the twin structure using polarized light microscopy. However, a detailed analysis of x-ray patterns[22] revealed heavy twinning in the basal plane with both crystallographic directions contributing about equally to the total intensity.

The lattice parameters determined in these crystals agree very well with published results on materials with an oxygen concentration close to 7 ($a=0.38227$ nm, $b=0.38872$ nm, $c=1.16802$ nm). This information together with the measured high transition temperatures and small transition widths as well as the rather small irreversibility of the magnetization curves (cf. below) is taken as an indication of the high quality of the present crystals.

B. Irradiation conditions

All the irradiations were made in the central irradiation facility of the TRIGA Mark-II reactor in Vienna, whose flux-density distribution has been established accurately.[23] At full reactor power, the flux density of fast neutrons amounts to 7.6×10^{16} m^{-2}s^{-1} ($E>0.1$ MeV). The sample temperature during irradiation is not known accurately, but is estimated from previous experiments to be less than 60 °C. During irradiation the crystals were kept under pure He atmosphere in a small sealed quartz cylinder, which was inserted into an open (i.e., pool-water-filled) aluminum container. Crystal *S*71 was sequentially irradiated to fluences of 2, 4, 8, and 12×10^{21} m^{-2} ($E>0.1$ MeV), *S*84 to 1 and 2×10^{22} m^{-2} ($E>0.1$ MeV). Following this high-fluence irradiation, the crystal broke after the first set of magnetization measurements; its fragments were then crushed further and used for transmission electron microscopy.[19]

C. Magnetization measurements and evaluation procedures

The measurements of the transition curves, as well as complete magnetization cycles at constant temperature were taken using a noncommercial SQUID magnetometer (based on an SHE VTS 800), which is equipped with a superconducting 8-T magnet and covers temperatures between 2 and 400 K. In order to obtain the magnetic moments, the single crystals are moved continuously between a pair of compensated pickup coils, which provide the input signals of the SQUID sensor. Numerous problems, which may be related to the inhomogeneity of the magnetic field,[24,25] to drift effects, and to magnetic moments of sample holders, to flux jumps in the SQUID itself, etc., and which are, in general, inaccessible to peak-to-peak signal detection, have forced us to develop new signal processing and numerical evaluation procedures[26] and to completely abandon peak-to-peak detection. (Because the improvements were introduced only in the course of the present series of experiments, some earlier measurements are associated with larger experimental uncertainties than the later ones.)

TABLE I. Physical dimensions and transition temperatures of single crystals *S*71 and *S*84.

Sample	Dimensions			Transition temperature	
	a (mm)	b (mm)	c[a] (mm)	T_c (onset) (K)	ΔT_c (K)
*S*71	0.39	0.35	0.18	91.0	5.4
*S*84	0.40	0.30	0.16	92.2	4.5

[a] Determined from the weight and the theoretical density ($\rho=6.45$ g cm^{-3}).

The nominal sensitivity of the magnetometer is about 10^{-11} A m^2. Sensitivities better than 10^{-10} A m^2 have been observed routinely in the low-field measurements made to determine T_c. For these experiments, the system had to be warmed above the transition temperature of the NbTi magnet in order to enable "zero-field-cooled" or low-field Meissner experiments. At high fields (5–8 T), the sensitivity is worse, but has improved from $\sim 10^{-9}$ to $\sim 5\times 10^{-10}$ A m^2, due to the improved processing procedures.

The further evaluation may be summarized as follows. First, the moments are converted into magnetizations using the measured sample weight and the theoretical density of $YBa_2Cu_3O_7$. This was found to be more reliable than calculating the volume from the crystal dimensions. Second, corrections for demagnetization have to be employed, as described in much detail recently.[27] The actual demagnetization factors of each sample were determined in separate low-field experiments (5 K, 0–2 mT) from the slopes of the magnetization in fields parallel to the c axis and to the a,b plane, respectively. Since the results ($D^c \sim 0.5$, $D^{a,b}=0.25$) are consistent with calculated demagnetization factors[28] and because the thicknesses of the crystals in the c direction are sufficiently high, extreme thin-plate effects as discussed by Däumling and Larbalestier,[29] are not expected to play a role. Hence, the transformation $\mu_0 H_{\rm eff}=\mu_0 H_a - DM$ has been employed throughout the analysis. It should be noted, however, that this transformation is negligible for all measurements with the field parallel to the basal plane (because M is so small), but of explicit significance for the case $\mathbf{H}\|\mathbf{c}$, in particular, in order to determine the applicability range of the Bean model.[30]

Lastly, the critical current densities were evaluated from the magnetization curves using an extended Bean model.[31,27] These calculations are based on considering, firstly, the finite rectangular shape of the crystals[32] and, secondly, by accounting for the anisotropy of critical currents in high-T_c single crystals. In the case of heavily twinned single crystals and for fields $\mathbf{H}\|\mathbf{c}$, the critical current densities flowing in the basal plane are assumed to be isotropic (we will denote them by J_c^a further on). For $\mathbf{H}\|(a,b)$ and under the assumption that the critical current flowing along the a or (b) direction is identical to the j_c^a determined from the $\mathbf{H}\|\mathbf{c}$ experiment, the critical current density flowing along the c direction (J_c^c) can be extracted from the magnetization curve. This procedure, which is supported by the results of Ref. 31, was adopted throughout the whole analysis.

III. RESULTS

A. Transition temperatures

The transition temperatures were measured after each irradiation step by cooling the crystals in zero field to 5 K, applying a field of 1.6 mT parallel to the c axis, and measuring the moments at several temperatures up to T_c. The results for crystal $S71$ are shown in Fig. 1. Onset and "saturation" temperatures were determined by calculating tangents on both sides of the transitions. The corresponding results are listed in Table II. It will be noted that T_c initially decreases approximately linearly with neutron fluence, in agreement with previous results.[4] The widths of the transition curves increase slightly, but the measured heights remain unchanged. This seems to indicate that large regions of rather undamaged superconducting material exist even after irradiation to the highest fluences. The decrease of T_c itself is attributed to oxygen displacements.[33,34]

B. Magnetization

Results of magnetization measurements taken at constant temperature are shown in Fig. 2 as examples of data obtained on the two single crystals at different neutron fluences, temperatures, and field orientations. In all cases, the magnetization is plotted versus the effective field $H_{\rm eff}$. The general feature which has been observed throughout all the experiments in the range of neutron fluences covered, is a significant increase of irreversibility in the magnetization. This becomes particularly obvious for magnetization measurements with H parallel to the basal plane and at higher temperatures. Also, it should be noted that the maxima of the magnetization curves, which are indicative of the full flux penetration field H^* in the Bean model,[30] are shifted to considerably higher fields in the irradiated state. This imposes additional limitations on the field range accessible for Bean model evaluations in terms of critical current densities. Based on a careful analysis of experimental uncertainties associated with the magnetization data, we will restrict ourselves in the following to results obtained at low temperatures [$T=5$, 20, and 40 K for $\mathbf{H}\|\mathbf{c}$, and $T=5$ and 20 K for $\mathbf{H}\|(a,b)$], but include 77 K for $\mathbf{H}\|\mathbf{c}$ measured in the remanent state after a complete magnetization cycle to 8T.

C. Critical current densities

The principal effects of neutron irradiation on critical current densities are summarized in Fig. 3, where the

TABLE II. Transition temperatures and widths as a function of fast neutron fluence.

$S71$ fluence (m^{-2}, $E>0.1$ MeV)	0	2×10^{21}	4×10^{21}	8×10^{21}	12×10^{21}
T_c (K)	91.0	90.9	90.7	88.6	87.1
ΔT_c (K)	5.4	6.2			7.0

$S84$ fluence (m^{-2}, $E>0.1$ MeV)	0	10×10^{21}
T_c (K)	92.2	88.0
ΔT_c (K)	4.5	7.0

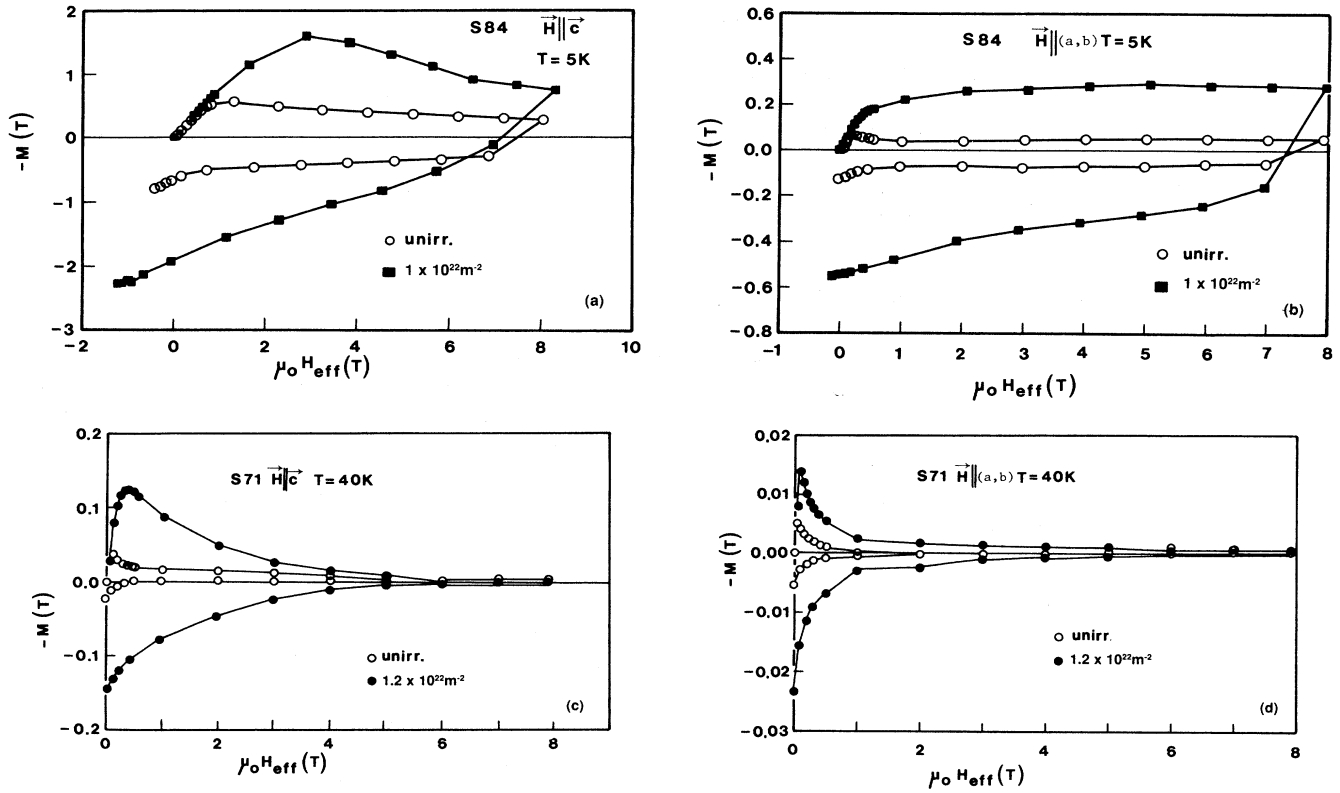

FIG. 2. Magnetization curves measured on samples *S*84 and *S*71. (a) *S*84: $T=5$ K, $\mu_0\mathbf{H}\|\mathbf{c}$ and $\|(a,b)$, unirradiated and at 1×10^{22} m^{-2}; (b) *S*71: $T=40$ K, $\mu_0\mathbf{H}\|\mathbf{c}$ and $\|(a,b)$, unirradiated and at 1.2×10^{22} m^{-2}.

critical current densities in the basal plane (J_c^a) and along the c direction (J_c^c) are plotted versus neutron fluence at fixed low temperature (5 K) and at fixed magnetic field (2 T). For both crystals, significant enhancements of J_c are observed. However, the rate of this enhancement becomes smaller with increasing neutron fluence and tends to show characteristic structures, in particular for $\mathbf{H}\|(a,b)$. At the same time, the anisotropy of critical current densities becomes much smaller [Fig. 3(c)]. Both crystals—although from the same batch—behave very differently already in the unirradiated state (the anisotropy factors being 175 and 14, respectively), and the reduction factors of J_c anisotropy at a fluence of 10^{22} m^{-2} are 4 and 2, respectively.

An overview of the J_c dependence on fluence is shown in Fig. 4 for crystal *S*71 at 20 K. For $\mathbf{H}\|\mathbf{c}$, kinks start to develop at high fields and relatively low fluences ($>2\times10^{21}$ m^{-2}). For $\mathbf{H}\|(a,b)$, similar effects occur initially, but the current densities are nearly independent of field and tend to increase again at the highest fluence. Raising the temperature (Fig. 5) leads to a fluence dependence which is comparable to the one observed at lower temperatures and high fields, i.e., kinks develop at a fluence of 2×10^{21} m^{-2} followed by subsequent enhancements of J_c, in particular for $\mathbf{H}\|(a,b)$.

Clearly, the fluence dependence of J_c at different fields and temperatures is not as straightforward as would be expected from a simple defect-production consideration. It should be pointed out, however, that similar complicated fluence dependences have been observed on conventional superconductors previously.[13,35,36] They have been attributed to the interaction of the neutron-induced defects with the preexisting defect structure as well as the neutron-induced changes of the primary superconductive properties of the materials, such as T_c, H_{c2}, etc. Attempts to discuss the present data in terms of these considerations are deferred to Sec. IV.

As a final remark we wish to emphasize the role of neutron-induced defects on the temperature dependence of J_c. Data obtained on both crystals after a full magnetization cycle to 8 T and back to zero field are shown in Fig. 6 for $\mathbf{H}\|\mathbf{c}$. If the critical current densities in the remanent state are compared at 5 and 77 K, the enhancement factors are 2.8 and 12 for crystal *S*84, and 3.6 and 23 for crystal *S*71. Bearing in mind that the J_c values of *S*84 prior to irradiation had been considerably larger than for crystal *S*71, these different enhancement factors are consistent with the general observation that radiation-induced flux-pinning effects are inversely correlated to the preirradiation J_c's. (Note also that our previously reported[4] enhancement factors of ~3 at 77 K were obtained on single crystals with preirradiation J_c's of about 1 order of magnitude higher than the present ones.) Most importantly, however, the data of Fig. 6 demonstrate that the slopes of the temperature dependence of J_c are changed in a characteristic way, which seems to indi-

cate that the newly introduced defects exert stronger pinning forces at higher temperatures, i.e., have "deeper" pinning potentials than the preirradiation defects.

D. Volume-pinning forces

In view of the large number of parameters involved in the discussion of radiation effects on the superconductive properties of the single crystals, an attempt is made in this section to arrive at a more uniform presentation by employing calculated values of the volume-pinning forces $\mathbf{P}_v = \mathbf{J}_c \times \mathbf{B}$. An appropriate analysis would require plots of P_v versus reduced induction $b = B/\mu_0 H_{c2}$. However, since the upper critical fields are neither known in the unirradiated state nor as a function of neutron fluence, we have to restrict ourselves to a presentation of pinning forces versus induction B, as shown in Figs. 7–9.

Again, the two crystals $S84$ and $S71$ behave rather differently. In Fig. 7 we note large increases of P_v at low temperatures as well as at 40 K, but reach the first observable maximum of P_v only for $\mu_0\mathbf{H}\|\mathbf{c}$ at 40 K, a field of 6 T, and a neutron fluence of 1×10^{22} m^{-2}. On the contrary, maxima of the P_v curves are observed at all temperatures and fluences in crystal $S71$ for $\mathbf{H}\|\mathbf{c}$ (Fig. 8). These maxima increase in all cases with neutron fluence, but shift initially to lower fields and then again to higher fields at the highest fluences ($8-12\times10^{21}$ m^{-2}). No com-

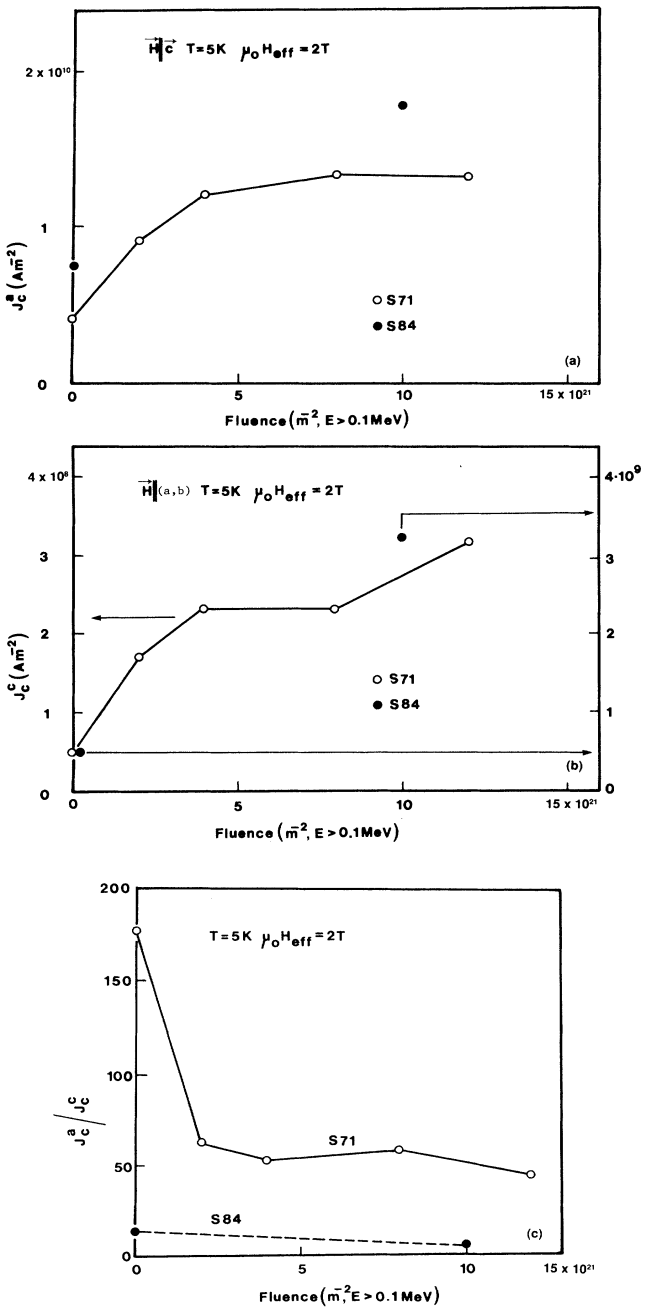

FIG. 3. Fluence dependence of critical current densities in both single crystals measured at 5 K. (a) $\mu_0\mathbf{H}\|\mathbf{c}$; (b) $\mu_0\mathbf{H}\|(a,b)$; (c) ratio of critical current densities J_c^a/J_c^c as a function of neutron fluence.

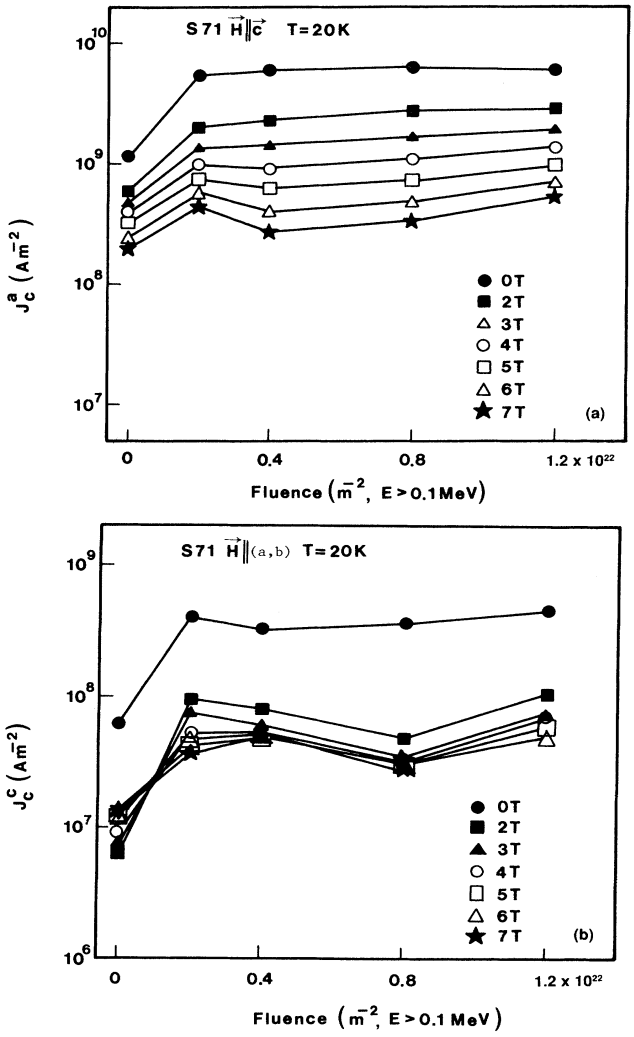

FIG. 4. Fluence dependence of critical current densities at a fixed temperature of 20 K, but for effective fields between 0 and 7 T. (a) $\mu_0\mathbf{H}\|\mathbf{c}$; (b) $\mu_0\mathbf{H}\|(a,b)$.

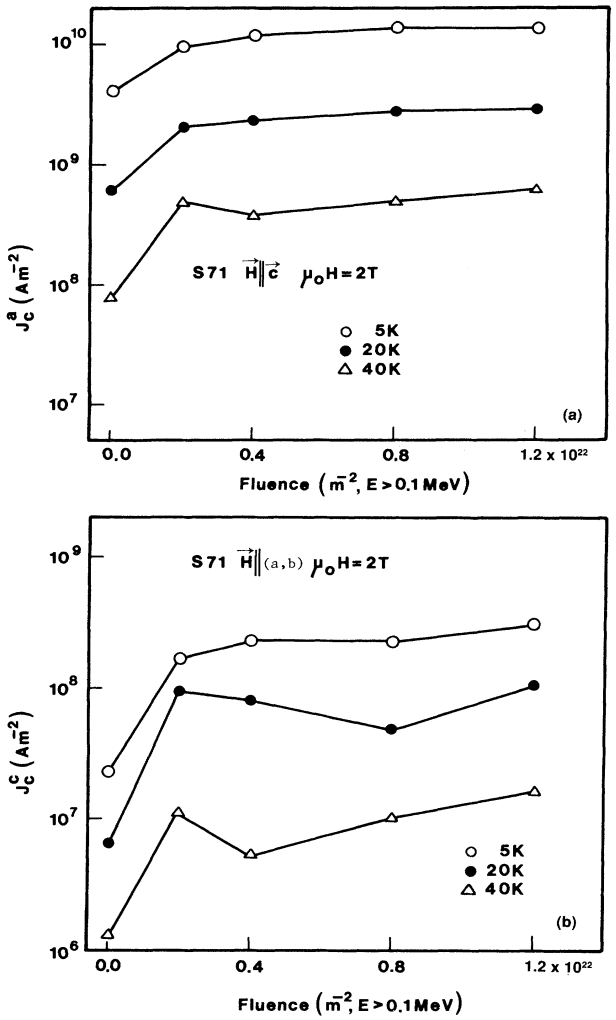

FIG. 5. Fluence dependence of critical current densities at a fixed field of 2 T, but for different temperatures (5, 20, and 40 K). (a) $\mu_0\mathbf{H}\|\mathbf{c}$; (b) $\mu_0\mathbf{H}\|(a,b)$.

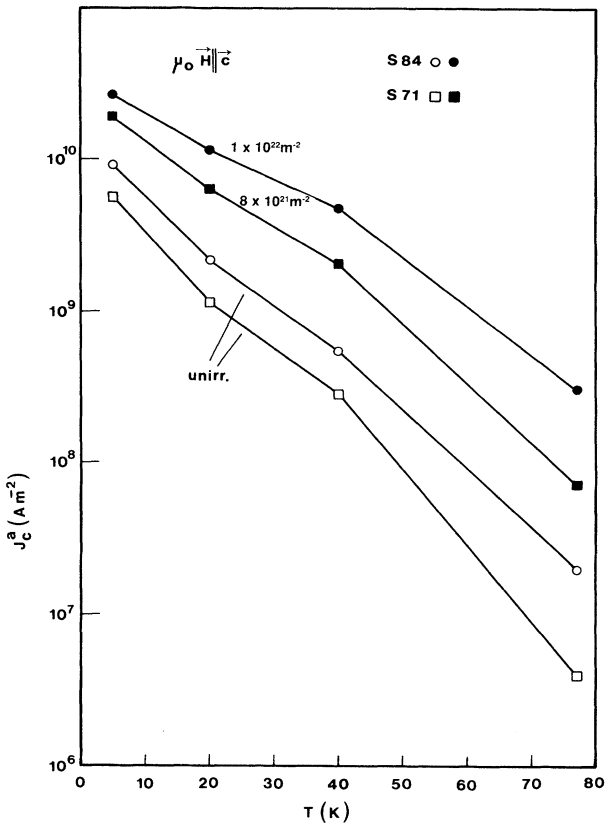

FIG. 6. Temperature dependence of critical current densities in the remanent state after a full magnetization cycle to 8 T ($\mu_0\mathbf{H}\|\mathbf{c}$). Pre- and postirradiation data are compared (*S*71: 8×10^{21} m^{-2}, *S*84: 1×10^{22} m^2).

parable effects are observed for $\mathbf{H}\|(a,b)$ (Fig. 9), although the data come close to the limits of our resolution (shaded area).

The increase of P_v is, of course, again the signature of an enhanced pinning action of the radiation-induced defects. A shift of the maximum to lower fields usually indicates the action of less pinning centers (unless the upper critical field H_{c2} is strongly reduced), whereas a shift to higher fields would indicate the appearance of more pinning centers.[32] Hence, the data presented in Figs. 7–9 strongly suggest that the interplay of the newly created defects with the preirradiation defect structure plays the key role in the radiation effects observed on $YBa_2Cu_3O_{7-\delta}$ single crystals.

IV. DISCUSSION

A discussion of these results must necessarily be qualitative in nature at the present time, since many of the basic parameters, such as the radiation-induced changes of H_{c2}, are not known. However, it should be pointed out that—although the crystals showed different magnetization behavior prior to irradiation—the *relative changes* of J_c with neutron fluence and with respect to the preirradiation conditions are consistent. Based on this conclusion, we have to invoke two counteracting mechanisms in the following discussion in order to explain the data in a qualitative way.

According to recent experiments by Welp *et al.*,[37] a significant contribution to flux pinning stems from the twin boundaries, which also act as traps for other point defects in the crystal.[38,39] In addition, a certain amount of stress is still expected to exist in these areas, which may also contribute to flux pinning.[40] The radiation-induced defects will certainly interact with this (preirradiation) defect structure.

Transmission electron microscopy has been used to obtain preliminary information on the nature of these defects.[19,41] Following 50-keV Xe irradiation (which was selected because of the similar defect production compared to fast neutrons), relatively large (~5 nm) collision cascades have been observed which, in some cases, were found to consist of recrystallized superconducting material, but misoriented by as much as 10°–30° compared to

the original crystal orientation. These defects are certainly able to act as strong additional pinning centers. Secondly, transmission electron microscopy has been employed on crystal *S*84 after exposure to a neutron fluence of 2×10^{22} m^{-2}.[19] In this case, large areas of highly defective or amorphous material were found to be embedded in 10–30-nm regions of relatively undisturbed superconductor. Clearly, at this fluence level the defects have become too big and too overlapped in order to still exert individual basic pinning forces on the flux lines, in particular, at the relatively low flux-line densities prevailing at our highest fields (the equilibrium flux lattice spacing at 8 T amounts to ~15 nm). Thirdly, however, neutrons with energies below 0.1 MeV, which usually do not contribute to the cascade production, will certainly be able to produce additional point defects. These defects, which can be neglected in conventional superconductors because of their large coherence lengths, may either act as additional pinning centers in the high T_c's or strengthen the preirradiation defect structure by accumulating in the defective

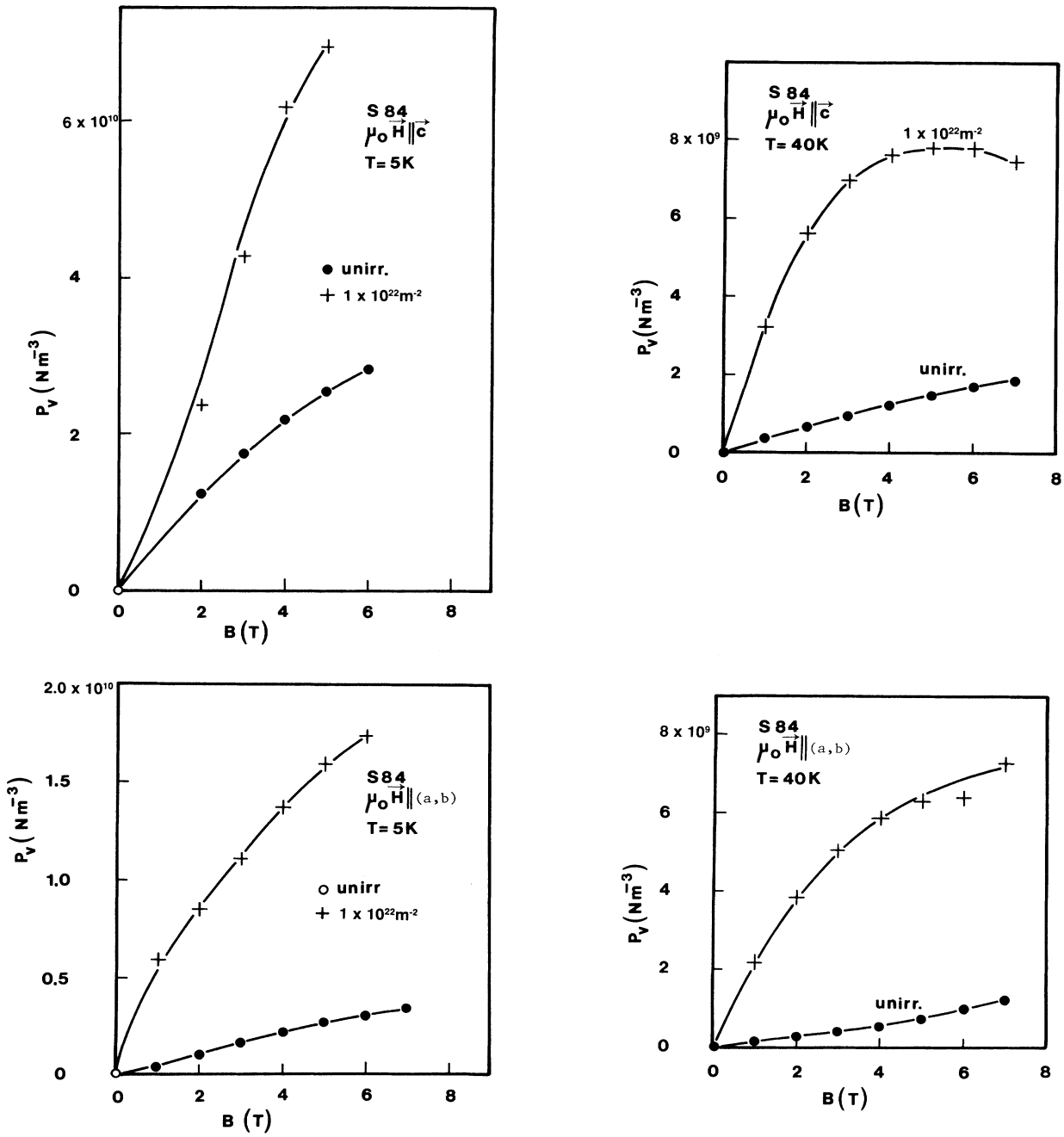

FIG. 7. Volume-pinning forces P_v as a function of induction B in single crystal *S*84 prior to and following irradiation to 1×10^{22} m^{-2}. Left-hand side: $T=5$ K; right-hand side: $T=40$ K.

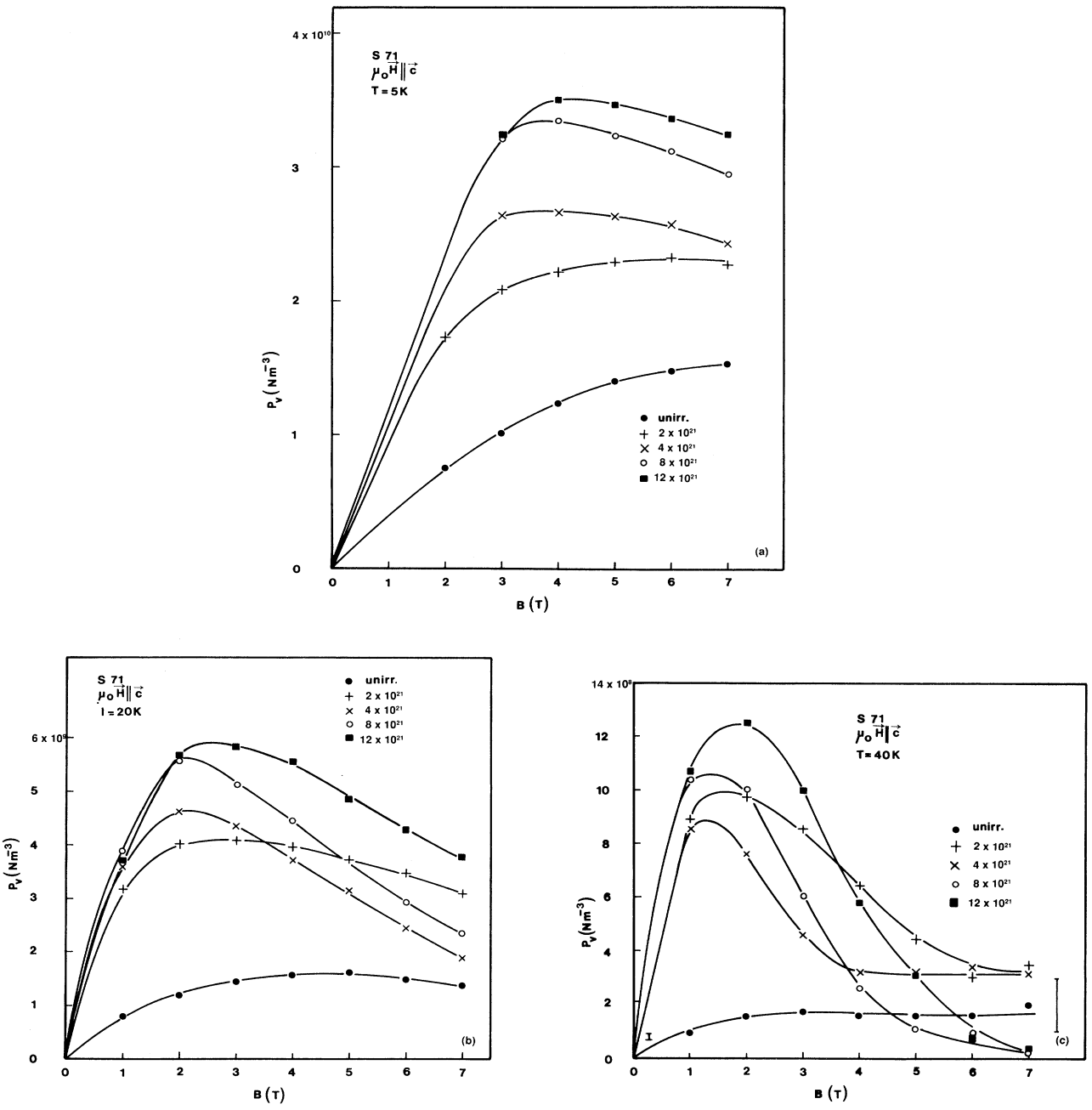

FIG. 8. Volume-pinning forces P_v as a function of induction B in single crystal $S71$ for $\mu_0 \mathbf{H} \| \mathbf{c}$. Parameter of the curves is the fast neutron fluence. (a) $T = 5$ K; (b) $T = 20$ K; (c) $T = 40$ K.

areas around the twins during the defect formation.

Hence, from all of these considerations we expect a large increase of flux pinning at low neutron fluences. However, with increasing fluence and a linearly increasing number of defects, the effectiveness of these pinning centers is expected to decrease for the following reasons. Firstly, as seen in the electron micrographs and as mentioned above, the primary collision cascades introduced into the undisturbed superconducting material begin to overlap and, therefore, are unable to further enhance the pinning forces. The fluence level, at which this process sets in is not known yet, but is presently being investigated by electron microscopy in a systematic way.[42] Secondly, the probability of producing a cascade at the location of an already existing pinning center increases with increasing neutron fluence. Hence, preirradiation defects disappear and are partly replaced by new ones. Thirdly, defect processes which have been found to lead to a par-

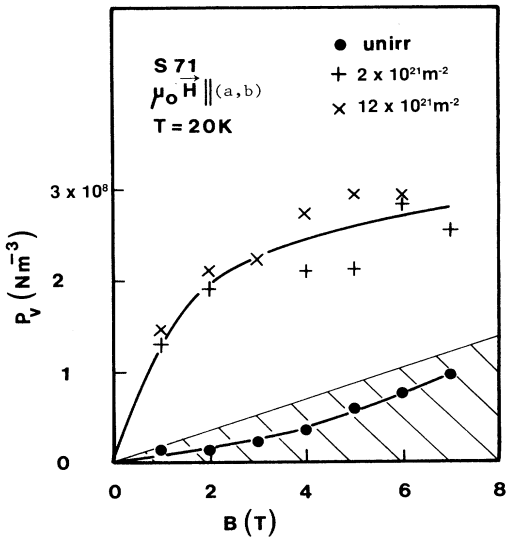

FIG. 9. Volume-pinning forces P_v as a function of induction B in single crystal $S71$ for $\mu_0\mathbf{H}\|(a,b)$ at 20 K. The shaded area indicates the resolution limits of the present experiment.

tial recrystallization of the superconductor will certainly be able to relieve the internal strain around the twin boundaries and, hence, also reduce possible pinning forces based on this mechanism. At the same time, this recrystallization under different orientations could very well account for the large reduction of flux-pinning anisotropy [Fig. 3(c)], in particular, at low fluence levels.

A more detailed discussion of results, which could account for the nonlinear enhancement of flux pinning with neutron fluences and for the large differences in radiation response observed for the two single crystals, cannot be given at the present stage. Further experiments involving higher-resolution magnetization measurements (on larger crystals), lower neutron fluences and, in particular, more information on the preirradiation defect structures and the radiation-induced changes of H_{c2} are currently under way.[43]

CONCLUSIONS

We have presented a systematic study of fast neutron irradiation effects on critical current densities and flux pinning. The results have been deduced from magnetization measurements on two high-quality YBCO single crystals in the temperature range from 5 to 77 K, for magnetic fields up to 8 T, and for field orientations parallel to the c axis and the a,b plane, respectively. All the evaluations have been made within the framework of an extended anisotropic Bean model.

In contrast to all previous work, the *same* crystals have been investigated prior to and following irradiation, which enables us to directly analyze the results as a function of neutron fluence and of the preirradiation pinning strength. The main conclusions can be summarized as follows:

(1) Neutron irradiation leads to large increases of critical current densities and pinning forces.

(2) The enhancements of J_c are larger at higher temperatures. Although no quantitative evaluations of the pinning potentials U_0 could be made because of the lack of sufficient information on the relaxation of the magnetization, this temperature dependence (Fig. 6) of the enhancement factors strongly suggests that the radiation-induced defects have deeper pinning potentials than the preirradiation flux-pinning centers. The search for other "suitable" defects is, therefore, encouraged by these results.

(3) The anisotropy of critical current densities is strongly reduced with neutron fluence. This observation can be related to the completely isotropic and homogeneous exposure of the superconductor to the radiation and, consequently, to a homogeneous defect production. In addition, high-resolution electron microscopy of defect cascades has revealed recrystallization processes under large tilting angles, which could immediately explain the effective loss of anisotropy.

(4) The dependence of critical current densities and pinning forces on neutron fluence varies between samples. According to the discussion presented in Sec. IV, this effect is attributed to the interaction of the radiation-induced defects with the preirradiation defect structure, which is known to vary significantly from single crystal to single crystal.

(5) At higher neutron fluences, the enhancement of flux pinning becomes much less pronounced. Based on electron-microscopy results on one of the crystals irradiated to a fluence of 2×10^{22} m^{-2}, we note that the defects have become too large (5–10 nm) compared to a flux line core ($\lesssim$2 nm) and too dense compared to the flux line spacing at our highest field ($\sim$15 nm) in order to still act as effective pinning centers.

Further work will be needed to clarify details of the observed radiation response of these high-T_c single crystals.

ACKNOWLEDGMENTS

We wish to thank H. Niedermaier (Wien) for his technical help with the experiments, Dr. M. A. Kirk and Dr. L. R. Greenwood (Argonne) for most valuable discussions and M. C. Frischherz (Argonne/Wien) for communicating his results prior to publication. This work was supported in part by Fonds zur Förderung der Wissenschaftlichen Forschung, Wien, under Contract No. 6837 and by the U. S. Department of Energy, Basic Energy Sciences, Material Sciences, under Contract No. W-31-109-ENG-38.

[1]S. Jin, H. Tiefel, R. C. Sherwood, R. B. van Dover, M. E. Davis, G. W. Kammlott, and R. A. Fastnacht, Phys. Rev. B **37**, 7850 (1989).
[2]M. Murakami, M. Morita, K. Doi, and K. Miyamoto, Jpn. J. Appl. Phys. **28**, 1189 (1989).
[3]K. Salama, V. Selvamanickam, L. Gao, and K. Sun, Appl. Phys. Lett. **54**, 2352 (1989).
[4]A. Umezawa, G. W. Crabtree, J. Z. Liu, H. W. Weber, W. K. Kwok, L. H. Nunez, T. J. Moran, and C. H. Sowers, Phys. Rev. B **36**, 7151 (1987).
[5]H. W. Weber, G. W. Crabtree, A. Umezawa, J. Z. Liu, and L. H. Nunez, in *High-T_c Superconductors,* edited by H. W. Weber (Plenum, New York, 1988), p. 273.
[6]H. W. Weber, in *Studies of High Temperature Superconductors,* edited by A. Narlikar (Nova Science, New York, 1989), p. 197.
[7]F. M. Sauerzopf, H. P. Wiesinger, H. W. Weber, G. W. Crabtree, and J. Z. Liu, Physica C **162-164**, 751 (1989).
[8]Proceedings of the International Discussion Meeting on Radiation Effects on Superconductivity, Argonne, IL, 1977, edited by B. S. Brown, H. C. Freyhardt, and T. H. Blewitt [J. Nucl. Mat. **72** (1978)].
[9]Proceedings of the International Conference on Neutron Irradiation Effects in Solids, Argonne, IL, 1981, edited by M. A. Kirk [J. Nucl. Mat. **108&109** (1982)].
[10]A. R. Sweedler, C. L. Snead, Jr., and D. E. Cox, in *Treatise on Materials Science and Technology,* Volume 14 of *Metallurgy of Superconducting Materials,* edited by T. Luhman and D. Dew-Hughes (Academic, New York, 1979), p. 349.
[11]H. R. Kerchner, R. R. Coltman, Jr., C. E. Klabunde, and S. T. Sekula, J. Nucl. Mat. **72**, 233 (1978).
[12]H. W. Weber, Adv. Cryog. Eng. **32**, 853 (1986).
[13]H. W. Weber, Kerntechnik **53**, 189 (1989).
[14]R. B. van Dover, E. M. Gyorgy, L. F. Schneemeyer, J. W. Mitchell, K. V. Rao, R. Puzniak, and J. V. Waszczak, Nature **342**, 55 (1989).
[15]H. Küpfer, I. Apfelstedt, W. Schauer, R. Flükiger, R. Meier-Hirmer, H. Wühl, and H. Scheurer, Z. Phys. B **69**, 167 (1987).
[16]S. T. Sekula, D. K. Christen, H. R. Kerchner, J. R. Thompson, L. A. Boatner, and B. C. Sales, Jpn. J. Appl. Phys. Suppl. **26-3**, 1185 (1987).
[17]A. Wisniewski, M. Baran, P. Przyslupski, H. Szymczak, A. Pajaczkowska, B. Pytel, and K. Pytel, Solid State Commun. **65**, 577 (1988).
[18]J. R. Cost, J. O. Willis, J. D. Thompson, and D. E. Peterson, Phys. Rev. B **37**, 1563 (1988).
[19]M. A. Kirk, M. C. Frischherz, J. Z. Liu, L. R. Greenwood, and H. W. Weber, Philos. Mag. Lett. **62**, 41 (1990).
[20]D. L. Kaiser, F. Holtzberg, M. F. Chisholm, and T. K. Worthington, J. Cryst. Growth **85**, 593 (1987).
[21]U. Welp, W. K. Kwok, G. W. Crabtree, K. G. Vandervoort, and J. Z. Liu, Phys. Rev. Lett. **62**, 1908 (1989).
[22]K. Mereiter (unpublished).
[23]H. W. Weber, H. Böck, E. Unfried, and L. R. Greenwood, J. Nucl. Mat. **137**, 236 (1986).
[24]G. M. Stollmann, B. Dam, J. H. P. Emmen, and J. Pankert, Physica C **159**, 854 (1989).
[25]G. M. Stollmann, B. Dam, J. H. P. Emmen, and J. Pankert, Physica C **161**, 444 (1989).
[26]W. Kritscha, F. M. Sauerzopf, and H. W. Weber, Physica B **165&166**, 109 (1990).
[27]F. M. Sauerzopf, H. P. Wiesinger, and H. W. Weber, Cryogenics **30**, 650 (1990).
[28]J. A. Osborn, Phys. Rev. **67**, 351 (1945).
[29]M. Däumling and D. C. Larbalestier, Phys. Rev. B **40**, 9350 (1989).
[30]C. P. Bean, Rev. Mod. Phys. **36**, 31 (1964).
[31]E. M. Gyorgy, R. B. van Dover, K. A. Jackson, L. F. Schneemeyer, and J. V. Waseczak, Appl. Phys. Lett. **55**, 283 (1989).
[32]A. M. Campbell and J. E. Evetts, *Critical Currents in Superconductors* (Taylor & Francis, London, 1972).
[33]M. A. Kirk, M. C. Baker, J. Z. Liu, D. J. Lam, and H. W. Weber, in *High-T_c Superconductors* (Ref. 5), p. 59.
[34]M. A. Kirk, M. C. Baker, J. Z. Liu, D. J. Lam, and H. W. Weber, Mat. Res. Soc. Symp. Proc. **99**, 209 (1988).
[35]F. Nardai, H. W. Weber, and R. K. Maix, Cryogenics **21**, 223 (1981).
[36]P. Gregshammer, H. W. Weber, R. T. Kampwirth, and K. E. Gray, J. Appl. Phys. **64**, 1301 (1988).
[37]U. Welp, W. K. Kwok, G. W. Crabtree, K. G. Vandervoort, and J. Z. Liu, Appl. Phys. Lett. **57**, 84 (1990).
[38]Y. Zhou, M. Suenaga, Y. Xu, R. L. Sabatini, and A. R. Moodenbaugh, Appl. Phys. Lett. **54**, 374 (1989).
[39]P. Pongratz (private communication).
[40]J. Z. Liu (private communication).
[41]M. A. Kirk, M. C. Frischherz, J. Z. Liu, and H. W. Weber (unpublished).
[42]M. C. Frischherz (unpublished).
[43]H. P. Wiesinger (unpublished).